Dynamic Simulation of Industrial Poly(vinyl chloride) Batch Suspension Polymerization Reactors

C. Kiparissides,* G. Daskalakis, D. S. Achilias, and E. Sidiropoulou

Chemical Engineering Department and Chemical Process Engineering Research Institute, Aristotle University of Thessaloniki, P.O. Box 472, 540 06 Thessaloniki, Greece

In the present study a comprehensive mathematical model is developed to simulate the dynamic behavior of industrial poly(vinyl chloride) (PVC) batch suspension polymerization reactors. More specifically, the model predicts the monomer concentration in the gas, aqueous, and polymer phases, the overall monomer conversion, the polymerization rate and polymer chain structural characteristics (e.g., number- and weight-average molecular weights, long-chain branching, short-chain branching, and number of terminal double bonds), the reactor temperature and pressure, and the jacket inlet and outlet temperatures over the whole polymerization cycle. An experimental reactor is employed to verify the theoretical model predictions. It is shown that experimental results on the time evolution of reactor temperature and pressure, the jacket inlet and outlet temperature, and the final conversion and molecular weight averages are in very good agreement with model predictions. The predictive capabilities of the model are also demonstrated through the simulation of experimental data recently reported in the literature. Finally some results on the optimization of the PVC production are presented.

Introduction

Poly(vinyl chloride) (PVC) is one of the oldest polymers and the second largest in volume thermoplastic manufactured in the world (Smallwood, 1990). The actual demand in Western Europe for PVC in 1992 was 5.2 million tons, and the forecast for 1999 is estimated at 6 million tons (Bevis, 1996). The enormous expansion of the PVC industry is due to the high versatility of PVC as a plastic raw material together with its low price. A review of the qualitative and quantitative aspects of PVC polymerization can be found in Burgess (1982), Langsam (1986), and Törnell (1988) and more recently in Smallwood (1990), Xie et al. (1991a,b), and Yuan et al. (1991).

Approximately 75% of the world's PVC is produced by the suspension polymerization process. According to this technique, droplets of liquid vinyl chloride monomer (VCM) containing oil-soluble initiator(s) are dispersed in the continuous aqueous phase by a combination of strong stirring and the use of suspending agents (stabilizers). The reaction takes place in the suspension droplets. For modeling purposes, each droplet can be treated as a small batch bulk polymerization reactor. VCM, which boils at −13.4 °C, is normally polymerized in a batch reactor by dispersing the liquid monomer, under pressure, in water, in a well-stirred jacketed reactor. The reactor's contents are heated to the required temperature where the initiator(s) start(s) to decompose and polymerization begins. The heat of polymerization is transferred from the monomer droplets to the aqueous phase and then to the reactor wall, which is cooled by chilled water flowing through the reactor's jacket. When all the free liquid monomer has been used up, the pressure in the reactor starts to fall as a result of the monomer mass transfer from the vapor phase to the polymer phase due to subsaturation conditions. In industrial PVC production, the reaction is usually stopped when a certain pressure drop has been recorded. Since PVC is effectively insoluble in its own monomer, once the polymer chains are first generated, they precipitate immediately to form two separate phases in the polymerizing droplet. From a kinetic point of view the polymerization of VCM is considered to take place in three stages.

Stage 1. During the first stage, primary radicals formed by the thermal fragmentation of initiator rapidly react with monomer molecules to produce PVC macromolecules which are insoluble in the monomer phase. The reaction mixture consists mainly of pure monomer, since the polymer concentration is less than its solubility limit (conversion $\leq 0.1\%$).

Stage 2. This stage extends from the time of appearance of the separate polymer phase to a fractional conversion, X_f, at which the separate monomer phase disappears. The reaction mixture consists of four phases, namely, the monomer-rich phase, the polymer-rich phase, the aqueous phase, and the gaseous phase. The reaction takes place in the monomer and polymer phases at different rates and is accompanied by transfer of monomer from the monomer phase to the polymer phase so that the latter is kept saturated with monomer. The disappearance of the monomer phase is associated with a pressure drop in the reactor.

Stage 3. Finally, at higher conversions ($X_f < X < 1.0$) only the polymer-rich phase swollen with monomer exists. The monomer mass fraction in the polymer phase decreases as the total monomer conversion approaches a final limiting value.

The operational objective in an industrial PVC suspension polymerization process is to produce resins with desired molecular and morphological properties in a safe and efficient way, that can be handled and processed easily. This means that the polymer must consistently meet the required product specifications. Therefore, there is a strong incentive to develop comprehensive mathematical models capable of predicting the reactor behavior as well as the development of molecular properties during the course of polymerization.

* Author to whom correspondence should be addressed. Telephone: 31-996211, 31-996212. Fax: 31-996198, 31-980160. E-mail: CYPRESS@ALEXANDROS.CPERI.FORTH.GR.

S0888-5885(96)00483-6 CCC: $14.00

In the past several mathematical models have been developed to describe the two-phase suspension polymerization of VCM (Abdel-Alim and Hamielec, 1972; Kuchanov and Bort, 1973; Ray et al., 1975; Ugelstad et al., 1981; Chan et al., 1982; Hamielec et al., 1982; Kelsall and Maitland, 1983; Weickert et al., 1987a,b, 1988a,b; Xie et al., 1991b−d; Bretelle and Machietto, 1994; Dimian et al., 1995; Lewin, 1996). These have been recently reviewed by Sidiropoulou and Kiparissides (1990) and Yuan et al. (1991). However, due to the complexity of physical and chemical phenomena taking place in the reactor, each publication treats only a special aspect of the process (e.g., reaction kinetics, phase equilibria, etc.). Actually, there is a limited number of papers dealing with the development of comprehensive, quantitative models describing the reactor dynamics in terms of the process conditions. Therefore, the aim of the present study is to develop a detailed mathematical model to simulate the dynamic behavior of industrial PVC batch suspension polymerization reactors.

The present paper has been organized as follows: In the subsequent section, the polymerization kinetics are reviewed. Based on a detailed kinetic mechanism, general rate functions for the production of "live" and "dead" polymer chains are derived. The method of moments is invoked to recast the infinite set of macromolecular species balance equations into a lower order system of ordinary differential equations describing the molecular property developments in the polymer reactor. Three additional structural characteristics of the polymer chains related to the number of long- and short-chain branches and the number of terminal double bonds are identified and calculated during the reaction.

In the third part of the paper, detailed material balance equations are derived to predict the time evolution of the initiator, monomer, and inhibitor during the whole course of the reaction.

Energy balances for the reaction mixture and heating/cooling fluids are also derived to calculate the reactor temperature, together with the jacket inlet, outlet, and metal wall temperatures as a function of the polymerization time.

Phase equilibria are the subject of the next section. Fundamental thermodynamic equations are derived for the calculation of monomer concentration in the different phases and the prediction of the reactor pressure under both isobaric and nonisobaric conditions. The quantification of diffusion-controlled termination and propagation reactions is examined in a subsequent section. Gel-effect and glass-effect phenomena are treated using a fundamental model proposed by Achilias and Kiparissides (1992).

The experimental suspension polymerization reactor system (Voutetakis, 1992) is briefly described in the last section of the paper. Finally, a comparison of model predictions with some experimental data is presented. It is shown that experimental results on the time evolution of reactor temperature and pressure, as well as on final conversion and molecular weight averages, are in very good agreement with theoretical predictions. Furthermore, the predictive capabilities of the present model are demonstrated by comparison of the model predictions with some recent experimental data published in the literature. Last but not least, certain important conclusions regarding the optimization of the PVC reactor are drawn.

It should be noted that, to our knowledge, this is the first comprehensive model combining reaction kinetics with detailed material and energy balances and reactor phase equilibria to simulate the dynamic behavior of batch PVC suspension polymerization reactors. The benefits of this model can be illustrated in view of its industrial application.

Reaction Kinetics and Molecular Property Equations

The free-radical VCM suspension polymerization mechanism includes the following elementary reactions (Hamielec et al., 1982; Sidiropoulou and Kiparissides, 1990; Xie et al., 1991b):

Initiation:

$$\mathrm{I}_{i,j} \xrightarrow{k_{\mathrm{d}_{i,j}}} 2\mathrm{I}^{\bullet}_{i,j}; \qquad i = 1, 2, ..., N_{\mathrm{d}} \tag{1}$$

$$\mathrm{I}^{\bullet}_{i,j} + \mathrm{M}_j \xrightarrow{k_{\mathrm{I}_{i,j}}} \mathrm{R}^{\bullet}_{1,j} \tag{2}$$

Propagation:

$$\mathrm{R}^{\bullet}_{x,j} + \mathrm{M}_j \xrightarrow{k_{\mathrm{p}_j}} \mathrm{R}^{\bullet}_{x+1,j} \tag{3}$$

Chain transfer to monomer:

$$\mathrm{R}^{\bullet}_{x,j} + \mathrm{M}_j \xrightarrow{k_{\mathrm{fm}_j}} \mathrm{P}_x + \mathrm{R}^{\bullet}_{1,j} \tag{4}$$

Chain transfer to polymer:

$$\mathrm{R}^{\bullet}_{x,2} + \mathrm{P}_y \xrightarrow{k_{\mathrm{fp}_2}} \mathrm{P}_x + \mathrm{R}^{\bullet}_{y,2} \tag{5}$$

Intramolecular transfer (backbiting):

$$\mathrm{R}^{\bullet}_{x,j} \xrightarrow{k_{\mathrm{b}_j}} \mathrm{R}^{\bullet}_{x,j} \tag{6}$$

Termination by disproportionation:

$$\mathrm{R}^{\bullet}_{x,j} + \mathrm{R}^{\bullet}_{y,j} \xrightarrow{k_{\mathrm{td}_j}} \mathrm{P}_x + \mathrm{P}_y \tag{7}$$

Termination by combination:

$$\mathrm{R}^{\bullet}_{x,j} + \mathrm{R}^{\bullet}_{y,j} \xrightarrow{k_{\mathrm{tc}_j}} \mathrm{P}_{x+y} \tag{8}$$

Inhibition:

$$\mathrm{R}^{\bullet}_{x,j} + \mathrm{Z}_j \xrightarrow{k_{\mathrm{z}_j}} \mathrm{P}_x + \mathrm{Z}^{\bullet}_j \tag{9}$$

$$\mathrm{Z}^{\bullet}_j + \mathrm{Z}^{\bullet}_j \xrightarrow{k_{\mathrm{Zt}_j}} \mathrm{Z}_j + \text{inactive products} \tag{10}$$

In the above kinetic scheme, the symbols I, Z, and M denote the initiator, inhibitor, and monomer molecules, respectively. Radicals formed by the fragmentation of the initiator and the inhibition reaction are denoted by the symbols $\mathrm{I}^{\bullet}$ and $\mathrm{Z}^{\bullet}$, respectively. N_{d} stands for the number of initiators used in the polymerization. The symbols $\mathrm{R}^{\bullet}_x$ and P_x are used to identify the respective live macroradicals and the dead polymer chains, containing x monomer units. It should be noted that all the above elementary reactions but the chain transfer to polymer can take place either in the monomer phase ($j = 1$) and/or in the polymer phase ($j = 2$).

To simplify the derivation of the dynamic molar balance equations describing the conservation of the various live and dead polymer chains, the following assumptions are made: (i) Polymerization of VCM in the water and vapor phases is negligible. (ii) Polymerization of VCM proceeds in one phase (monomer-rich) when conversion is less than 0.1%, in two phases (e.g., monomer-rich and polymer-rich) in the conversion range $0.1 < X < X_f$, and in one phase (polymer-rich) at higher than X_f values of conversion. (iii) No transfer of radicals between the two phases occurs. (iv) Equilibrium partition of monomer, initiator(s), and inhibitor between the monomer-rich and the polymer-rich phase is assumed at all times. (v) All the kinetic rate constants are independent of the polymer chain length. (vi) The quasi-steady-state approximation is only applied to the primary radicals. (vii) No depropagation reactions occur.

Accordingly, based on the postulated kinetic mechanism and assumptions, the following general rate functions for the production of live and dead polymer chains are derived:

$$r_{R^{\bullet}_{x,j}} = (\sum_{i=1}^{N_d} 2f_{i,j}k_{d_{i,j}}[I]_{i,j} + k_{fm_j}[M]_j\sum_{y=1}^{\infty}[R^{\bullet}_{y,j}])\varphi_j\delta(x-1) + k_{p_j}[M]_j[R^{\bullet}_{x-1,j}]\varphi_j[1-\delta(x-1)] - \{(k_{p_j}+k_{fm_j})[M]_j + k_{Z_j}[Z]_j + (k_{tc_j}+k_{td_j})\sum_{y=1}^{\infty}[R^{\bullet}_{y,j}]\}[R^{\bullet}_{x,j}]\varphi_j + (k_{fp_2}x[P_x]\sum_{y=1}^{\infty}[R^{\bullet}_{y,j}] - k_{fp_2}[R^{\bullet}_{x,j}]\sum_{y=1}^{\infty}y[P_y])\varphi_2(j-1) \quad (11)$$

$$r_{P_x} = \sum_{j=1}^{2}(k_{fm_j}[M]_j + k_{Z_j}[Z]_j + k_{td_j}\sum_{y=1}^{\infty}[R^{\bullet}_{y,j}])\varphi_j[R^{\bullet}_{x,j}] + \frac{1}{2}\sum_{j=1}^{2}k_{tc_j}\sum_{y=1}^{x-1}[R^{\bullet}_{y,j}][R^{\bullet}_{x-y,j}]\varphi_j - (k_{fp_2}x[P_x]\sum_{y=1}^{\infty}[R^{\bullet}_{y,j}] - k_{fp_2}[R^{\bullet}_{x,j}]\sum_{y=1}^{\infty}y[P_y])\varphi_2 \quad (12)$$

$\delta(x)$ is Kronecker's delta and is given by

$$\delta(x) = \begin{cases} 1 & \text{if } x = 0 \\ 0 & \text{if } x \neq 0 \end{cases} \quad (13)$$

$\varphi_j = V_j/V$ refers to the volume fraction of each phase.

Molecular Property Balances. To reduce the infinite system of molar balance equations, required to describe the molecular weight distribution developments, the method of moments is invoked (Achilias and Kiparissides, 1994). Accordingly, the average molecular properties of the polymer (i.e., M_n, M_w) are expressed in terms of the leading moments of the dead polymer molecular weight distribution. The moments of the total number chain length (TNCL) distributions of live radical and dead polymer chains are defined as

$$\lambda_{i,j} = \sum_{x=1}^{\infty}x^iR^{\bullet}_{x,j}; \qquad \mu_i = \sum_{x=1}^{\infty}x^iP_x; \qquad i = 0, 1, 2, \ldots \quad (14)$$

The corresponding moment rate functions are obtained by multiplying each term of eqs 11 and 12 by x^i and summing the resulting expressions over the total range of variation of x (Achilias and Kiparissides, 1994):

Live polymer moment equations

$$r_{\lambda_{i,j}} = \sum_{k=1}^{N_d}2f_{k,j}k_{d_{k,j}}[I]_{k,j}\varphi_j + k_{fm_j}[M]_j[\lambda_{0,j}]\varphi_j + k_{p_j}[M]_j\{\sum_{k=0}^{i}\binom{i}{k}[\lambda_{k,j}]\}\varphi_j - \{(k_{p_j}+k_{fm_j})[M]_j + k_{Z_j}[Z]_j + (k_{tc_j}+k_{td_j})[\lambda_{0,j}]\}[\lambda_{i,j}]\varphi_j + (k_{fp_2}[\lambda_{0,j}][\mu_{i+1}] - k_{fp_2}[\lambda_{i,j}][\mu_1])\varphi_2(j-1) \quad (15)$$

Dead polymer moment equations

$$r_{\mu_i} = \sum_{j=1}^{2}(k_{fm_j}[M]_j + k_{Z_j}[Z]_j + k_{td_j}[\lambda_{0,j}])[\lambda_{i,j}]\varphi_j + \frac{1}{2}\sum_{j=1}^{2}k_{tc_j}\sum_{k=0}^{i}\binom{i}{k}[\lambda_{k,j}][\lambda_{i-k,j}]\varphi_j - (k_{fp_2}[\lambda_{0,j}][\mu_{i+1}] - k_{fp_2}[\lambda_{i,j}][\mu_1])\varphi_2 \quad (16)$$

It should be pointed out that when transfer to polymer reactions is included in the kinetic mechanism, the n-order polymer moment equation will depend on the $(n+1)$-order moment. This is due to the fact that the transfer to polymer rate function depends on the total number of monomer units in the polymer chains. To break down the dependence of the moment equations on higher order moments, several closure methods have been proposed. In the present investigation, the method of the so-called "bulk" moments is used. According to this closure method (Arriola, 1989; Baltsas et al., 1996), a bulk moment $\mu_i + \lambda_{i,1} + \lambda_{i,2}$ is defined which includes the contribution of the live polymer chains. Notice that the term $\mu_i + \lambda_{i,1} + \lambda_{i,2}$ can be approximately μ_i due to the insignificant contribution of the $\lambda_{i,1}$ and $\lambda_{i,2}$ terms. Thus, by adding the second-order live radical moment equations to the second-order dead polymer moment equation, one can obtain the following expression for the bulk second-order moment

$$r_{(\mu_2+\lambda_{2,1}+\lambda_{2,2})} \approx r_{\mu_2} = \sum_{k=1}^{N_d}\sum_{j=1}^{2}2f_{k,j}k_{d_{k,j}}[I]_{k,j}\varphi_j + 2\sum_{j=1}^{2}k_{p_j}[\lambda_{1,j}][M]_j\varphi_j + \sum_{j=1}^{2}k_{tc_j}[\lambda_{1,j}]^2\varphi_j + \sum_{j=1}^{2}(k_{p_j}+k_{fm_j})[\lambda_{0,j}][M]_j\varphi_j \quad (17)$$

Note that eq 17 is independent of the higher order moments (e.g., μ_3). The number- and weight-average molecular weights can be expressed in terms of the moments of the TNCLDs of live and dead polymer chains as follows:

Number-average molecular weight:

$$M_n = MW_m\frac{\mu_1 + \lambda_{1,1} + \lambda_{1,2}}{\mu_0 + \lambda_{0,1} + \lambda_{0,2}} \cong MW_m\frac{\mu_1}{\mu_0} \quad (18)$$

Weight-average molecular weight:

$$M_w = MW_m\frac{\mu_2 + \lambda_{2,1} + \lambda_{2,2}}{\mu_1 + \lambda_{1,1} + \lambda_{1,2}} \cong MW_m\frac{\mu_2}{\mu_1} \quad (19)$$

The polydispersity index (D), which is a measure of the breadth of the MWD, is defined as the ratio of the weight-average to the number-average molecular weight ($D = M_w/M_n$). Abdel-Alim and Hamielec (1972) and Xie

et al. (1991c) have also developed models for the calculation of the molecular weight averages and its distribution.

On the basis of the general kinetic scheme considered in this study (eqs 1−10), one can identify three additional structural characteristics of the polymer chains related to the number of long-chain branches (LCB), the number of short-chain branches (SCB), and the number of terminal double bonds (TDB). To calculate the time variation of LCB, SCB, and TDB per polymer molecule (e.g., L_n, S_n, and T_n, respectively), the following differential equations are considered:

$$\frac{d(LCB)}{dt} = \frac{d(L_n[\mu_0])}{dt} = k_{fp_2}[\lambda_{0,2}][\mu_1] \qquad (20)$$

$$\frac{d(SCB)}{dt} = \frac{d(S_n[\mu_0])}{dt} = \sum_{j=1}^{2} k_{b_j}[\lambda_{0,j}] \qquad (21)$$

$$\frac{d(TDB)}{dt} = \frac{d(T_n[\mu_0])}{dt} = \sum_{j=1}^{2} (k_{fm_j}[M]_j[\lambda_{0,j}] + k_{td_j}[\lambda_{0,j}]^2) \qquad (22)$$

The number density of LCB and the number density of SCB per 1000 monomer units are calculated from the following equations:

$$L_d = 1000\frac{L_n}{\mu_1/\mu_0}; \qquad S_d = 1000\frac{S_n}{\mu_1/\mu_0} \qquad (23)$$

Detailed Material and Energy Balances

Based on the kinetic mechanism considered in the previous section, the differential equations describing the time variation of initiator(s), inhibitor, and total monomer conversion are written as

$$\frac{dI_{i,j}}{dt} = -\sum_{j=1}^{2} k_{d_{i,j}} I_{i,j}; \qquad i = 1, 2, ..., N_d \qquad (24)$$

$$\frac{dZ_j}{dt} = -\frac{1}{2}\sum_{j=1}^{2} k_{Z_j} Z_j[\lambda_{0,j}] \qquad (25)$$

$$\frac{dX}{dt} = \sum_{j=1}^{2} k_{p_j}\frac{M_j}{M_0}[\lambda_{0,j}] \qquad (26)$$

In eqs 24−26 the subscript j refers to the monomer ($j = 1$) and polymer ($j = 2$) phases.

Energy Balances. The batch suspension polymerization reactor considered in the present study is schematically shown in Figure 1. It consists of a well-mixed jacketed vessel. Stirring is provided by a flat-blade turbine, aided by four removable blade baffles. The reaction temperature is controlled by a cascade controller which manipulates the flows of two streams (e.g., a hot and a cold) entering the reactor jacket. The energy balances for the reaction mixture, metal wall, and jacket fluid are subsequently formulated (Kiparissides and Shah, 1983):

(a) Reactor Mixture. Perfect mixing is assumed.

$$V_{mix}\rho_{mix}c_{\rho_{mix}}\frac{dT}{dt} = (-\Delta H_r)M_0\frac{dX}{dt} - h_iA_i(T - T_{met}) + F_w c_{p_w}\rho_w(T_a - T_0) - U_tA_t(T - T_a) \qquad (27)$$

where F_w represents the mass flow rate of the water

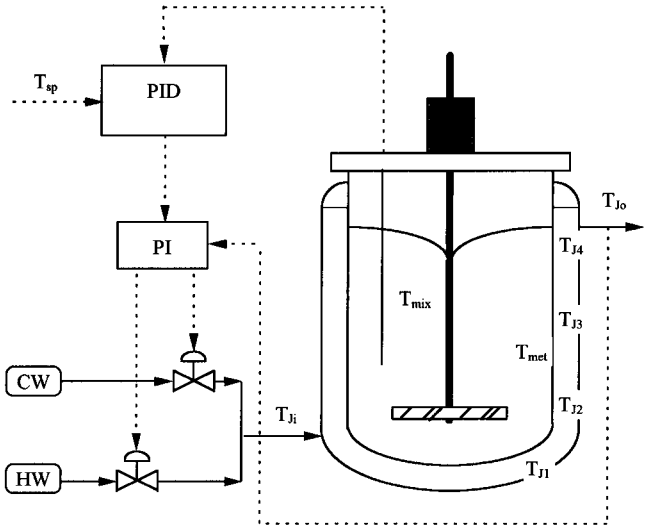

Figure 1. Experimental reactor system.

added in the reaction mixture during polymerization in order to maintain a constant liquid level. $T_0 = 0$ °C is a reference temperature. The term $U_tA_t(T - T_a)$ stands for the heat loss from the reactor top.

(b) Metal Wall. The reactor metal wall is treated as a lumped system.

$$V_{met}\rho_{met}c_{p_{met}}\frac{dT_{met}}{dt} = h_iA_i(T - T_{met}) - \frac{1}{4}A_0\sum_{i=1}^{4} h_{0,i}(T_{met} - T_{J,i}) \qquad (28)$$

(c) Jacket Fluid. The total jacket volume is divided into four zones of equal volume.

$$V_J\rho_{w,i}c_{p_{w,i}}\frac{1}{4}\frac{dT_{J,i}}{dt} = \frac{1}{4}h_{0,i}A_0(T_{met} - T_{J,i}) + \frac{1}{4}U_aA_a(T_a - T_{J,i}) + F_{w,J}c_{pw,i}\rho_{w,i}(T_{J,i-1} - T_{J,i}) \qquad (29)$$

Thermocouple System Dynamics. A first-order differential equation is employed to describe the time delay in temperature measurements.

$$\frac{dT_h}{dt} = \frac{1}{\tau_d}(T - T_h) \qquad (30)$$

where T_h is the temperature equivalent of the thermocouple output and τ_d is the delay constant.

Heat-Transfer Coefficients. Most correlations for the calculation of the inside film heat-transfer coefficient in agitated vessels are of the following general form:

$$Nu_i = \frac{h_iD_R}{k_{mix}} = F(Re_i)^a(Pr_i)^{1/3}\left(\frac{\mu_{mix}}{\mu_{mix,w}}\right)^b \qquad (31)$$

The values of the empirical parameters F, a, and b can be found in heat-transfer textbooks for different types of agitators. For a flat-blade turbine, the recommended values for these parameters are $F = 0.54$, $a = {}^2/_3$, and $b = 0.14$. Reynolds and Prandtl numbers appearing in eq 31 are defined as

$$Re_i = \frac{D_{imp}{}^2N_{imp}\rho_{mix}}{\mu_{mix}}; \qquad Pr_i = \frac{c_{p_{mix}}\mu_{mix}}{k_{mix}} \qquad (32)$$

where D_{imp} and N_{imp} denote the impeller diameter and revolution number, respectively.

The outside film jacket heat transfer coefficient can be calculated from the following equations depending on the jacket water flow conditions (e.g., laminar or turbulent):

Turbulent flow:

$$Nu_0 = \frac{h_0 D_{eq}}{k_w} = 0.023(Re_0)^{0.8}(Pr_0)^{1/3}\left(\frac{\mu_0}{\mu_w}\right)^{0.14} \quad (33)$$

Laminar flow:

$$Nu_0 = \frac{h_0 D_{eq}}{k_w} = 3.66 + \frac{0.085Gz}{1 + 0.047Gz^{2/3}}\left(\frac{\mu_0}{\mu_w}\right)^{0.14} \quad (34)$$

where the dimensional numbers used are defined as

$$Gz = (Re_0)(Pr_0)\frac{D_{eq}}{L_{eq}}; \qquad Pr_0 = \frac{c_{p_w}\mu_w}{k_w};$$

$$Re_0 = \frac{D_{eq}\rho_w u_w}{\mu_w} \quad (35)$$

D_{eq} and L_{eq} are the equivalent diameter and length, calculated in terms of the geometric characteristics of the reactor jacket. u_w stands for the water flow velocity in the jacket.

Controller Equations. A cascade control system consisting of a master PID and two slave PI controllers was employed to maintain the polymerization temperature within ±0.1 °C of the setpoint value by manipulating the cold and hot water flowrates to the reactor jacket. The master controller monitors the reaction temperature and its output drives the setpoint of the slave controller. The latter monitors the outlet temperature of the jacket fluid and drives the two separate control valves. To simulate the operation of the master and slave controllers, the following velocity form PID algorithms were utilized.

Master PID controller:

$$C_n = C_{n-1} + K_c\left[\left(1 + \frac{\tau}{\tau_i} + \frac{\tau_d}{\tau}\right)E_n - \left(1 + 2\frac{\tau_d}{\tau}\right)E_{n-1} + \frac{\tau_d}{\tau}E_{n-2}\right] \quad (36)$$

where $E_n = T_{sp} - T_h$ and 4 mA ≤ C_n ≤ 20 mA

Slave PI controller for cold water:

$$C_{n,c} = C_{n-1,c} + K_{cc}\left[\left(1 + \frac{\tau}{\tau_{ic}}\right)E'_n - E'_{n-1}\right] \quad (37)$$

Slave PI controller for hot water:

$$C_{n,h} = C_{n-1,h} - K_{ch}\left[\left(1 + \frac{\tau}{\tau_{ih}}\right)E'_n - E'_{n-1}\right] \quad (38)$$

where $E'_n = C_n - C'_n$ and C'_n is the mA equivalent of the $T_{j,4}$ (outlet jacket temperature) given by

$$C'_n = 4 + (16/100)(T_{j,4} - 273.16) \quad (39)$$

$C_{n,c}$ and $C_{n,h}$ are the slave control outputs varying in the range of 4−20 mA.

In addition to the above controller equations, one needs to provide the appropriate calibration curves for the valves relating the cold and the hot water flowrates to the corresponding slave controller outputs (Voutetakis, 1992).

Phase Equilibria Calculations

One of the major issues in the development of a comprehensive mathematical model for a suspension VCM polymerization reactor is the accurate prediction of the reactor pressure with respect to time under both isobaric and nonisobaric conditions. This requires a complete account of monomer distribution in the various phases (Xie et al., 1987). In the suspension VCM polymerization reactor, four different phases might exist, namely, the vapor, the aqueous, the monomer-rich, and the polymer-rich phases.

The vapor phase that occupies the free space on top of the liquid mixture in the reactor consists mainly of VCM and water vapor. The reactor pressure will be equal to the sum of VCM and water vapor partial pressures when a separate liquid monomer phase exists (e.g., $0 < X < X_f$). It should be noticed here that a small amount of residual air may be present in the overhead vapor phase. However, due to the very low vacuum typically applied in an industrial reactor (less than 0.1 bar), the amount of air can be assumed to be negligible. The aqueous phase consists of water and a small amount of VCM dissolved in it. The calculation of the VCM solubility is discussed in the following section. A separate monomer-rich phase is present in the polymerizing monomer droplets up to the critical monomer conversion, X_f. The disappearence of this phase is followed by a pressure drop in the reactor. The polymer-rich phase is saturated with monomer. During stage 2 of the polymerization, the monomer/polymer ratio remains constant, reflecting the equilibrium solubility of monomer in the polymer phase.

During polymerization the aforementioned four phases are assumed to be in equilibrium. As a result, the fugacities of VCM in the different phases will be equal:

$$\hat{f}^{\,g}_m = \hat{f}^{\,w}_m = \hat{f}^{\,m}_m = \hat{f}^{\,p}_m \quad (40)$$

Based on the above equilibrium assumption, the reactor pressure can be calculated through the following thermodynamic considerations. The fugacity coefficient, $\hat{\varphi}_m$, of VCM in the binary vapor mixture will be given by

$$\ln(\hat{\varphi}_m) = \ln\left(\frac{\hat{f}^{\,g}_m}{P_m}\right) = \ln\left(\frac{\hat{f}^{\,g}_m}{y_m P}\right) = \frac{P}{RT}[B_m + (1 - y_m)^2\delta_{mw}] \quad (41)$$

where

$$\delta_{mw} = 2B_{mw} - B_m - B_w \quad (42)$$

In eq 41 P denotes the total reactor pressure, B_i the second virial coefficient of the i component, and δ the monomer solubility. A detailed calculation of the virial coefficients appearing in eq 41 can be found in the appendix of this paper.

The mole fraction of VCM in the vapor phase, y_m, can be calculated from the corresponding mole fraction of water vapor, y_w, assuming that the water vapor partial pressure is equal to its saturation value:

$$y_m = (1 - y_w) = 1 - \frac{P^{sat}_w}{P} \quad (43)$$

During stage 2 of the polymerization, the monomer and the polymer phases are assumed to be in equilibrium. Accordingly, the monomer activity, α_m, can be computed from the Flory−Huggins equation:

$$\ln(\alpha_m) = \ln\left(\frac{\hat{f}_m^p}{f_m^0}\right) = \ln(1-\varphi_2) + \varphi_2 + \chi\varphi_2^2 \quad (44)$$

where φ_2 is the polymer volume fraction in the polymer-rich phase. A detailed calculation of the Flory−Huggins interaction parameter, χ, is presented in the appendix. The activity of VCM, α_m, will be given by the ratio of the monomer fugacity coefficient in the polymer phase over that in a standard state. The latter is assumed to be equal to the fugacity of the pure monomer at the reactor temperature and saturation pressure. Combining eqs 40, 41, and 44, one can obtain eqs 45 and 46 for the calculation of the total reactor pressure. It should

$$\hat{f}_m^p = \hat{f}_m^g \Rightarrow \alpha_m f_m^0 = \hat{\varphi}_m y_m P \quad (45)$$

$$f_m^0 \exp(\ln(1-\varphi_2) + \varphi_2 + \chi\varphi_2^2) = y_m P \exp\left(\frac{P}{RT}(B_m + (1-y_m)^2\delta_{mw})\right) \quad (46)$$

be noticed that, in the conversion range $0 < X < X_f$, the activity of VCM will be equal to 1. To estimate the critical value of $\varphi_{2,c}$, the value of α_m in eq 44 is set equal to 1.

$$0 = \ln(1-\varphi_{2,c}) + \varphi_{2,c} + \chi\varphi_{2,c}^2 \quad (47)$$

Calculation of the Monomer Distribution. In what follows detailed mass balance equations are derived for the calculation of the VCM distribution in the different phases (e.g., monomer, polymer, gaseous, and water). As mentioned in the Introduction, the VCM polymerization reaction is considered to take place in three stages.

Stage I: $0 < X < 0.001$. In the first stage, the monomer mass distributions in phases 1 (monomer-rich) and 2 (polymer-rich) will be equal to

$$M_1 = M_0(1-X) - M_{wat} - M_g; \qquad M_2 = 0 \quad (48)$$

Furthermore, the mass of monomer in the aqueous, M_{wat}, and gaseous phase, M_g, will be given by

$$M_{wat} = K\frac{P}{P_m^{sat}}W_{w1} \quad (49)$$

$$M_g = \frac{\hat{f}_m^g MW_m V_g}{RT} \quad (50)$$

where

$$W_{w1} = W_w - \frac{\hat{f}_w^g MW_w V_g}{RT} \quad (51)$$

$$V_g = \left[\frac{V_R - \frac{M_0}{\rho_m} - \frac{W_w}{\rho_w} + M_0 X\left(\frac{1}{\rho_m} - \frac{1}{\rho_p}\right)}{1 - \frac{1}{RT}\left(\frac{\hat{f}_m^g MW_m}{\rho_m} + \frac{\hat{f}_w^g MW_w}{\rho_w}\right)}\right] \quad (52)$$

In the above set of equations V_g, W_w, and W_{wl} denote the volume of the gaseous phase, the total mass of water initially introduced in the reactor, and the mass of water in the liquid phase, respectively. The VCM in water solubility constant, K, is set equal to 0.0088 (Nilsson et al., 1978). The fugacity of water in the gaseous phase, $\hat{f}_w^g$, will be given by the difference of the total reactor pressure, P, minus the monomer fugacity in the gaseous phase, $\hat{f}_m^g$, $\hat{f}_w^g = P - \hat{f}_m^g$.

Stage 2: $0.001 < X < X_f$. In the second stage, the monomer distribution in phases 1 and 2 will be given by the following set of equations:

$$M_1 = M_0\left(1 - \frac{X}{X_S}\right) - M_{wat} - M_g \quad (53)$$

$$M_2 = M_0\frac{X}{X_S}(1 - X_S) \quad (54)$$

$$X_S = \frac{\varphi_2\rho_p}{\varphi_2\rho_p + (1-\varphi_2)\rho_m} \quad (55)$$

M_{wat} and M_g are calculated by eqs 49−52. The concentration of monomer in each phase will remain constant and will be given by

$$[M_1] = \frac{\rho_m}{MW_m}; \qquad [M_2] = \frac{M_2}{MW_m V_2} \quad (56)$$

Finally, the volume of every phase will be given by

$$V_1 = M_1/\rho_m; \qquad V_2 = M_2/\rho_m + M_0 X/\rho_p \quad (57)$$

Stage 3: $X_f < X$. In the third stage, the monomer-rich phase disappears and the polymerization takes place only in the polymer-rich phase under monomer starvation conditions. Accordingly, the monomer distribution in the two phases takes the following form:

$$M_1 = 0; \qquad M_2 = M_0(1-X) - M_{wat} - M_g \quad (58)$$

$$M_g = \frac{\hat{f}_m^g MW_m}{RT}\left(V_g(X_f) + M_0(X - X_S)\left(\frac{1}{\rho_m} - \frac{1}{\rho_p}\right)\right) \quad (59)$$

The mass of monomer in the water phase, M_{wat}, is calculated from eqs 49 and 51.

Calculation of the Critical Conversion, X_f. The critical conversion where the separate monomer phase disappears, X_f, can be calculated from eq 53 by setting $M_1 = 0$.

$$X_f = \frac{X_S\left(M_0 - KW_{w1} - \frac{\hat{f}_m^g MW_m(V_R - M_0/\rho_m - W_w/\rho_w)}{[RT - (\hat{f}_m^g MW_m/\rho_m + \hat{f}_w^g MW_w/\rho_w)]}\right)}{M_0\left(1 + \frac{\hat{f}_m^g MW_m X_S(1/\rho_m - 1/\rho_p)}{[RT - (\hat{f}_m^g MW_m/\rho_m + \hat{f}_w^g MW_w/\rho_w)]}\right)} \quad (60)$$

Diffusion-Controlled Reactions

Diffusion-controlled phenomena affecting the termination and propagation reactions occurring in the polymer-rich phase are quantitatively described based on a theoretical model developed by Achilias and Kiparissides (1992). According to this model, the termination and propagation rate constants are expressed in terms of a reaction-limited term and a diffusion-limited one. The latter depends on the diffusion coefficients of the corresponding species (i.e., polymer and monomer) and an effective reaction radius. Furthermore, the so-

called "reaction diffusion" taking place at very high monomer conversions is also taken into account.

Diffusion-Controlled Termination Rate Constant. On the basis of this modeling approach, the termination rate constant is expressed as the sum of two terms, one taking into account the effect of diffusion of polymer chains, k_{tD}, and the other describing the so-called "residual termination" or reaction diffusion, $k_{t,res}$.

$$k_{t2} = k_{tD} + k_{t,res} \tag{61}$$

The first term in the right-hand side of eq 61 is subsequently expressed in terms of the intrinsic termination rate constant, k_{t0}, which is equal to the termination rate constant in the monomer-rich phase, k_{t1}, and the diffusion coefficient of the polymer, D_p, in the polymer-rich phase:

$$\frac{1}{k_{tD}} = \frac{1}{k_{t0}} + \frac{r_t^2}{3}\frac{\lambda_{0,2}}{D_p} \tag{62}$$

where r_t is the termination radius, given by

$$r_t = \frac{\left[\ln\left(\frac{1000\tau^3}{N_A\lambda_{0,2}\pi^{3/2}}\right)\right]^{1/2}}{\tau} \tag{63}$$

$$\tau = (3/2j_c\delta^2)^{1/2} \tag{64}$$

D_p is the polymer self-diffusion coefficient and is calculated from the extended free-volume theory of Vrentas and Duda (Achilias and Kiparissides, 1992):

$$D_p = \frac{D_{p0}}{M_w^2}\exp\left(-\gamma\frac{\omega_m\hat{V}_m^* + \omega_p\hat{V}_p^*\xi}{\xi\hat{V}_f}\right) \tag{65}$$

with

$$\xi = \frac{\hat{V}_m^* M_{jm}}{\hat{V}_p^* M_{jp}} \tag{66}$$

and

$$\hat{V}_f = \omega_m\hat{V}_m^* V_{fm} + \omega_p\hat{V}_p^* V_{fp} \tag{67}$$

At very high monomer conversions, the self-diffusion coefficient of the polymer becomes very small, resulting in an unrealistically low value of k_t according to eq 62. The reason is that eq 65 does not account for the motion of the radical chains caused by the monomer propagation reaction. This phenomenon is known as residual termination or reaction diffusion. Several models have been proposed for the calculation of the residual termination rate constant, $k_{t,res}$ (Achilias and Kiparissides, 1992; Buback et al., 1994). All models assume that the residual termination rate constant is proportional to the frequency of monomer addition to the radical chain end. Thus, $k_{t,res}$ is written as

$$k_{t,res} = Ak_p[M] = Ak_p[M]_0(1 - X) \tag{68}$$

Using the volume-swept-out model, the final expression for the proportionality rate constant, A, becomes (Buback et al., 1994):

$$A = \pi\delta^3 j_c N_A \tag{69}$$

Equations similar to eqs 61−69 for modeling the effect of diffusion-controlled phenomena on the termination rate constant have been recently proposed by Tefera et al. (1994) and Panke (1995).

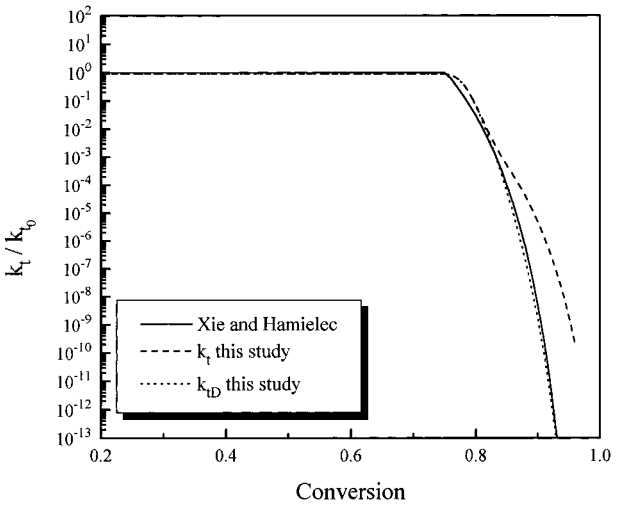

Figure 2. Termination rate constant versus conversion.

Diffusion-Controlled Propagation Rate Constant. Accordingly, k_{p2} can be expressed in terms of the intrinsic propagation rate constant, k_{p0}, (e.g., the propagation rate constant in the monomer-rich phase), and a diffusion term accounting for diffusional limitations of the propagation reaction.

$$\frac{1}{k_{p2}} = \frac{1}{k_{p0}} + \frac{1}{4\pi r_m N_A D_m} \tag{70}$$

Notice that the original equation (Achilias and Kiparissides, 1992) for the calculation of the propagation rate constant, k_{p2}, has been slightly modified according to comments made by Litvinenko and Kaminsky (1994). In eq 70, r_m denotes the radius of a monomer molecule. The monomer diffusion coefficient, D_m, is calculated from the extended free-volume theory of Vrentas and Duda (Achilias and Kiparissides, 1992):

$$D_m = D_{m0}\exp\left(-\gamma\frac{\omega_m\hat{V}_m^* + \omega_p\hat{V}_p^*\xi}{\hat{V}_f}\right) \tag{71}$$

All the symbols used in the preceding equations are explained in the Nomenclature section. All kinetic and transport parameters, appearing in eqs 61−71, have a clear physical meaning and can be calculated from available literature data (see the appendix).

The present model predictions on the variation of the termination and the propagation rate constants with respect to monomer conversion are compared in Figures 2 and 3 with the corresponding results obtained by the Xie et al. (1991b) model. It is appparent that both models show a similar behavior of k_t and k_p with monomer conversion.

Experimental and Simulation Results

Suspension polymerization experiments were carried out in a lab-scale automated batch reactor. The reactor system comprised an agitated 1-gal jacket vessel, a heating−cooling unit, a monomer feed unit, a sampling unit, a vacuum unit, a reaction termination unit, and a supervisory computer and process interface. Additional details about the design and operation of the reactor system can be found in Voutetakis (1992).

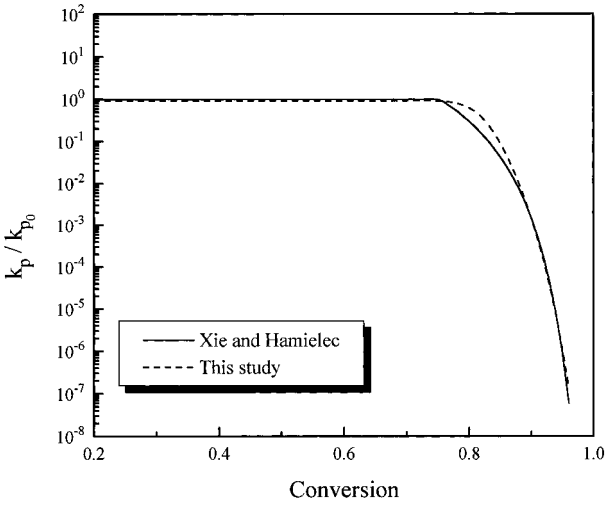

Figure 3. Propagation rate constant versus conversion.

A typical polymerization experiment involved the following steps: The reactor was initially filled with a known amount of distilled, deionized water in which the suspending agent was dissolved. Subsequently, a preweighed amount of initiator was added to the reactor, and the reactor pressure was reduced with the aid of a vacuum pump to about −10 psi. Afterward the VCM was pumped into the reactor, and the setpoint of the master controller was set to the polymerization temperature. The reactor temperature and pressure, as well as the jacket inlet and outlet temperatures and coolant flowrate, were continuously recorded using a computer-based data acquisition system. The final product was collected, and it was characterized according to its molecular weight distribution and particle size distribution. VCM of commercial grade was used in all experiments.

Several experiments were carried out to investigate the effect of polymerization temperature, type, and concentration of initiator(s), stabilizer type and concentration, impeller type and agitation rate on the molecular and morphological properties of the final product. A typical recipe comprised the following ingredients: monomer, 1.5−2 L; water, 1.5−2.4 L, initiator(s), 0.2−1.5 g/kg of VCM; stabilizer (e.g., Alcotex 72.5), 2 g/kg of VCM. The polymerization temperature was set to 60−65 °C.

The Reactor Simulator. A user-friendly software package that facilitates the production engineer to simulate the operation of industrial PVC suspension plants has been developed. Addressing this issue,

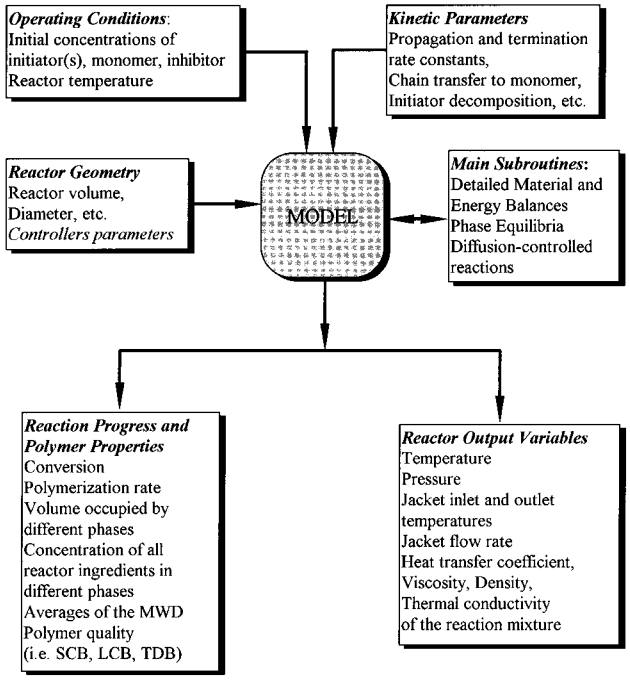

Figure 4. Logical diagram of the various input/output variables of the software package.

several input/output facilities have been built around the simulator that actually solves the problem (Pertsinidis et al., 1996). A schematic diagram presenting the main input−output functions of the simulator is shown in Figure 4. Four major categories of input data are required, namely, kinetic parameters, operating conditions, the reactor geometry, and the controller parameters. The model uses several subroutines to calculate the material and energy balances, reactor phase equilibria, and diffusional phenomena. The polymerization progress (e.g., conversion, rate, averages of the MWD, etc.) and reactor process variables (i.e., temperature profiles, pressure, etc.) can be obtained in either a tabulated or graphical form. The values of all kinetic, transport, and thermodynamic parameters used in the simulator are reported in Tables 1−4.

A typical simulated reaction profile, in terms of the time evolution of conversion, polymerization rate, reactor temperature, and pressure, is illustrated in Figure 5. The heat-up period (approximately 20 min) is characterized by an increase in the reactor's temperature and pressure. When the polymerization temperature reaches its specified setpoint value, the reaction actually begins and conversion and polymerization rate

Table 1. Physical Properties of Water, Monomer, and Polymer

physical property	water	VCM	PVC
density, ρ (kg/m^3)[a]	$1011.0 - 0.4484\theta$	$947.1 - 1.746\theta - 3.24 \times 10^{-3}\theta^2$	$10^3 \exp(0.4296 - 3.274 \times 10^{-4}T)$
heat capacity, c_p (kJ/kg K)[b]	$4.02 \exp(1.99 \times 10^{-4}T)$	$4.178(18.67 + 0.0758\theta)/62.5$	0.934[c]
viscosity, μ (kg/m min)[b]	$4.8 \exp(-1.5366 \times 10^{-2}T)$		
thermal conductivity, k (kJ/min m K)[b]	$8.212 \times 10^{-3} \ln(T) - 1.0661 \times 10^{-2}$		1×10^{-2} [c]

[a] Xie et al. (1991b). [b] Daupert and Danner (1985). [c] Burgess (1982).

Table 2. Thermodynamic Properties of Water and VCM (Daupert and Danner, 1985)

	water	VCM
vapor pressure, P^{sat} (Pa)	$\exp(72.55 - 7206.7/T - 7.1386 \ln(T) + 4.046 \times 10^{-6}T^2$	$\exp(126.85 - 5760.1/T - 17.914 \ln(T) + 2.4917 \times 10^{-2}T)$
accentric factor, ω	0.3342	0.1048
critical temperature, T_c (K)	647.5	432
critical pressure, P_c (bar)	220.5	56
critical volume, V_c (cm^3/mol)	56	179
critical compressibility factor, Z_c	0.233	0.283

Table 3. Reaction Kinetic Parameters

variable	value	units	ref
initiator: Perkadox 16-W40			*a*
MW	398	g/mol	
$k_{d_1} = k_{d_2}$	$2.31 \times 10^{15} \exp(-29100/RT)$	1/s	
$k_{p_1} = k_{p_2}$	$30 \times 10^{8} \exp(-3320/T)$	m^3/kmol/min	*b*
$k_{fm_1} = k_{fm_2}$	$5.78 \exp(-2768/T)k_{p_1}$	m^3/kmol/min	*b*
$k_{b_1} = k_{b_2}$	$0.014k_{p_1}$	min^{-1}	*b*
k_{fp_2}	$8.31 \times 10^{9} \exp(-11100/T)$	m^3/kmol/min	*a*
k_{t_1}	$2k_{p_1}^2/K_c$	m^3/kmol/min	
K_c	$6.08 \times 10^{-3} \exp(-5740(1/T - 1/T_0))$	m^3/kmol/min	*c*
$(k_{t_1}/k_{t_2})^{1/2}$	$24 \exp(1007(1/T - 1/T_0))$		*c*
T_0	333.15	K	
$(-\Delta H_r)$	106	kJ/kmol	*b*

[a] Xie et al. (1991b). [b] Sidiropoulou and Kiparissides (1990). [c] Our own laboratory.

Table 4. Parameters Used in the Diffusion Model

variable	value	units	ref
V_{fm}	$0.025 + a_m(T - T_{gm})$	cm^3/cm^3	
V_{fp}	$0.025 + a_p(T - T_{gp})$	cm^3/cm^3	
a_m	9.98×10^{-4}	K^{-1}	*a*
a_p	5.47×10^{-4}	K^{-1}	*a*
T_{gm}	70	K	*a*
T_{gp}	$87.1 - 0.132(T - 273.15)$	C	*a*
$\hat{V}_m^*$	0.7936	cm^3/g	*b*
$\hat{V}_p^*$	3.005	cm^3/g	*b*
ξ	0.375		*b*
γ	2		*b*
δ	6×10^{-10}	m	*c*
j_c	175		*c*

[a] Xie et al. (1991b). [b] Calculated in this study. [c] Ferry (1980).

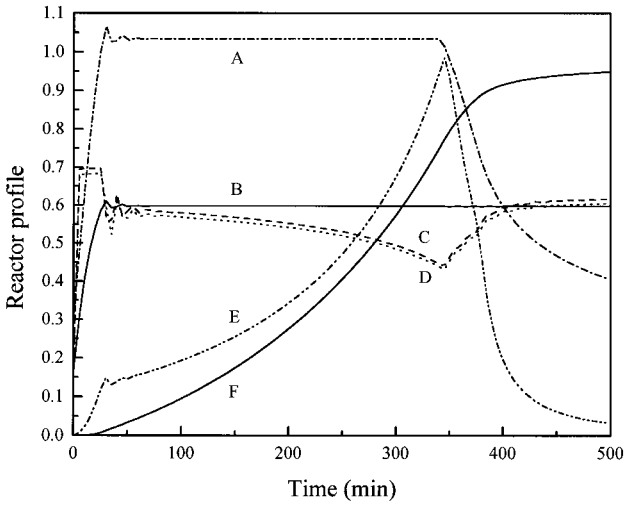

Figure 5. Typical output variables in a batch VCM suspension polymerization simulation: (A) reactor pressure in bar/10, (B) reactor temperature in °C/100, (C and D) jacket inlet and outlet temperatures, respectively, in °C/100, (E) polymerization rate in mol/L/min × 10, (F) monomer conversion.

increase. The effect of diffusion-controlled phenomena is denoted by a sharp increase in the polymerization rate, followed by an increase in reaction conversion. In order to maintain a constant reaction temperature, the jacket inlet temperature is considerably lowered. The peak in the reaction rate corresponds to the peak in the reaction exotherm (industrially usually called the "hot spot") and marks the onset of the pressure drop. After that point polymerization rate decreases considerably and the conversion slowly approaches its final value.

Results and Discussion

A comparison between model predictions and experimental data is provided in Figures 6 and 7. The reactor pressure (Figure 6) and the reactor and jacket inlet and

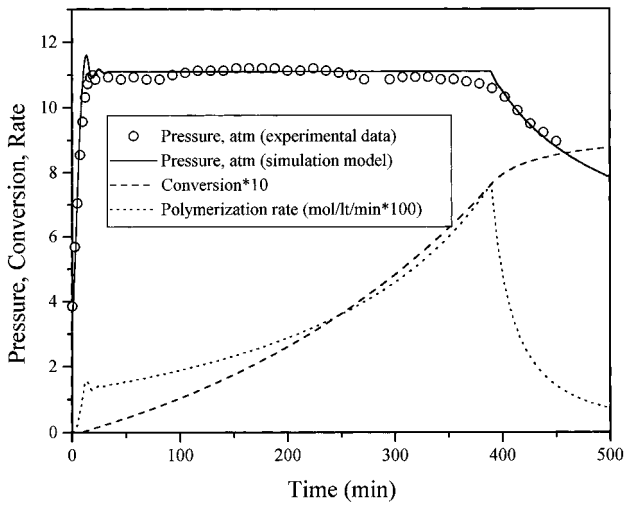

Figure 6. Comparison between theoretical and experimental reactor pressure values. Model predictions of conversion and polymerization rate with respect to time. Experimental conditions: T = 63 °C, initial reactor charge, 1.5 L of VCM, 1.5 L of water, and 1.57 g of dilauroyl peroxide/kg of VCM.

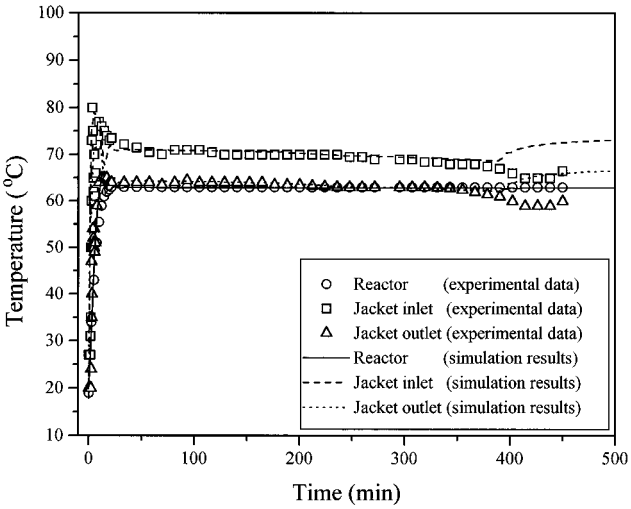

Figure 7. Comparison between model predictions and experimental measurements on reactor temperature and jacket inlet and outlet temperatures (experimental conditions as in Figure 6).

outlet temperatures obtained from the theoretical model are compared with experimental data. As can be seen, the model predictions are in good agreement with the experimental data. The calculated monomer conversion and reaction rate are also plotted in Figure 6.

In Figures 8 and 9 a comparison of model predictions and experimental data is provided for a typical polymerization carried out in the presence of a mixture of two initiators. As will be shown later in this section, a

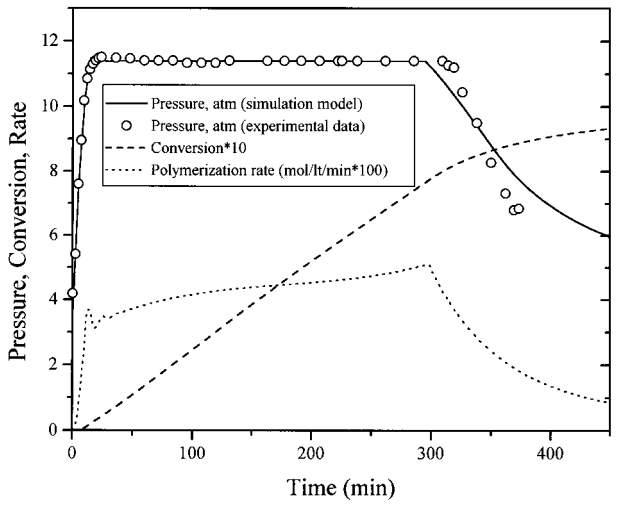

Figure 8. Comparison between theoretical and experimental reactor pressure values. Model predictions of conversion and polymerization rate with respect to time. Experimental conditions: $T = 64$ °C, initial reactor charge, 2.12 L of VCM, 2.34 L of water, 0.35 g of dilauroyl peroxide/kg of VCM, and 0.17 g of diethyl peroxydicarbonate/kg of VCM.

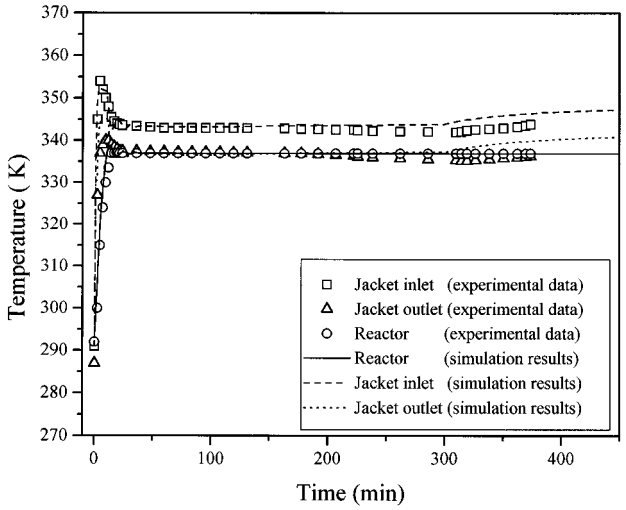

Figure 9. Comparison between theoretical model predictions and experimental measurements on reactor temperature and jacket inlet and outlet temperatures (experimental conditions as in Figure 8).

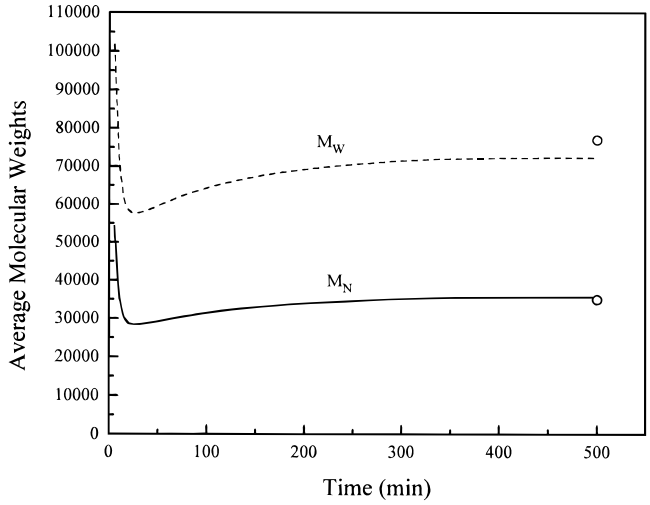

Figure 10. Predicted number- and weght-average molecular weight versus time. Circles represent final experimental measurements (experimental conditions as in Figure 8).

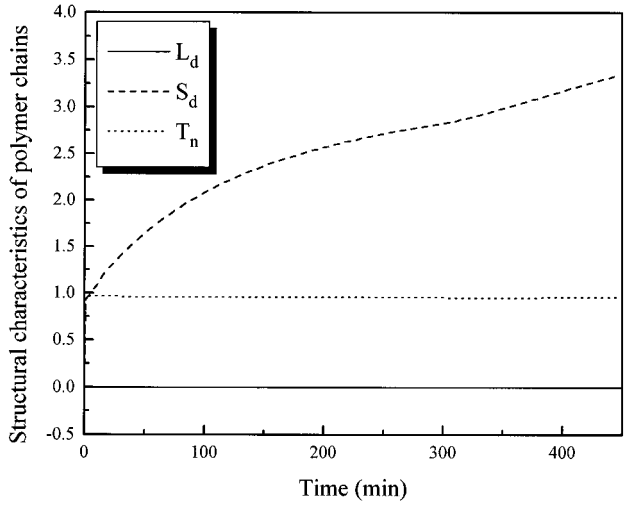

Figure 11. Molecular polymer properties versus time (experimental conditions as in Figure 8).

mixture of a slow and a fast initiator is often used to reduce the polymerization time by operating the reactor at an almost constant polymerization rate. Again a very good agreement between model predictions and experimental measurements is obtained. From Figure 8 one can notice that the combination of the two initiators results in a much smoother polymerization rate profile than the one plotted in Figure 6 (e.g., use of a single initiator).

The time histories of the molecular and structural characteristics of PVC predicted by the simulator are plotted in Figures 10 and 11. Experimental data on the final number- and weight-average molecular weights are in good agreement with the theoretical predictions. As is well-known (Smallwood, 1990), the molecular weight of PVC is mainly controlled by the polymerization temperature. Since the rate of chain termination is small, the average length of the polymer chains is determined by the ratio of the propagation rate to the rate of chain transfer to monomer, which is the dominant mechanism for chain termination. Thus, one can easily show that the polydispersity of the MWD will be close to 2.0. The initial increase in the average molecular weights observed in Figure 10 is due to the initial nonisothermal conditions. Concerning the structural characteristics of PVC, it should be pointed out that, although the number of long-chain branches per 1000 monomers, L_d, is very small (less than 10^{-3}), the number of short-chain branches, S_d, is on the order of 3. These results are in qualitative agreement with the experimental results of Scherrenberg et al. (1994). On the other hand, the number of terminal double bonds per polymer molecule remains almost constant at a value slightly less than 1. This is in accordance with the fact that the chain transfer to monomer reaction is the dominant termination reaction in VCM polymerization.

Figure 12 shows the monomer distribution in the different phases during the reaction. The monomer fraction in the monomer-rich phase decreases gradually with conversion until the critical conversion value X_f. At conversions greater than X_f the monomer concentration in the polymer-rich phase decreases gradually with time until the limiting conversion. In the imbedded figure the monomer fractions in the water and gaseous phases are plotted. Notice that, in the isobaric region, the amount of VCM in the aqueous phase remains constant and the amount in the gaseous phase increases due to the liquid volume contraction. In Figure 13 the time variations of the volume occupied by the monomer, polymer, and gaseous phases are plotted.

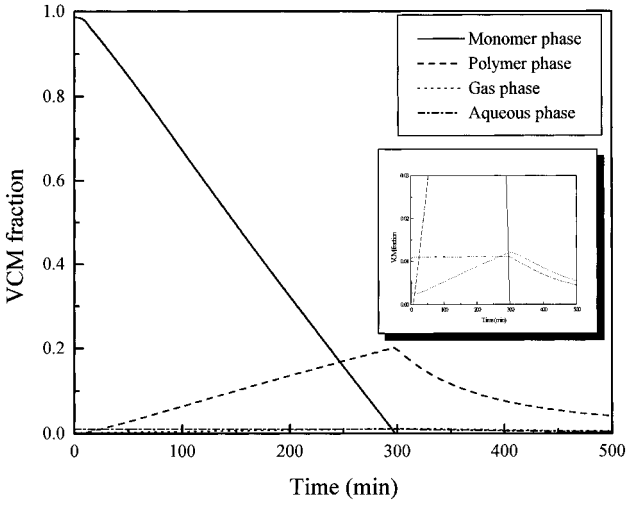

Figure 12. Monomer distribution in the different reaction phases (experimental conditions as in Figure 8).

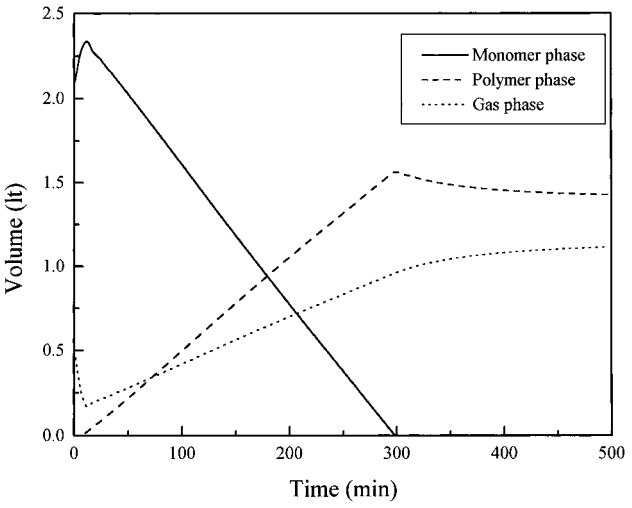

Figure 13. Volume occupied by the different phases in the reactor (experimental conditions as in Figure 8).

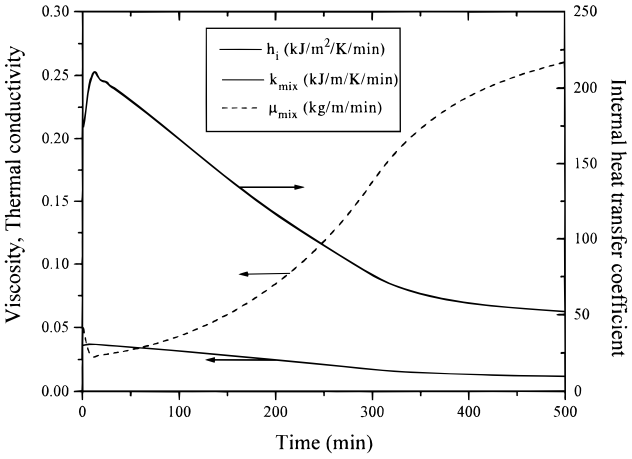

Figure 14. Variation of the physical and transport properties of the reaction mixture with time.

From a reactor design point of view it is interesting to follow the variation of the transport properties of the reaction mixture during the reaction (Figure 14). As can be seen, the reaction mixture viscosity increases with time roughly by an order of magnitude. As a result, the inside film heat-transfer coefficient to the metal wall decreases with time. The mixture thermal conductivity decreases also with the polymerization time.

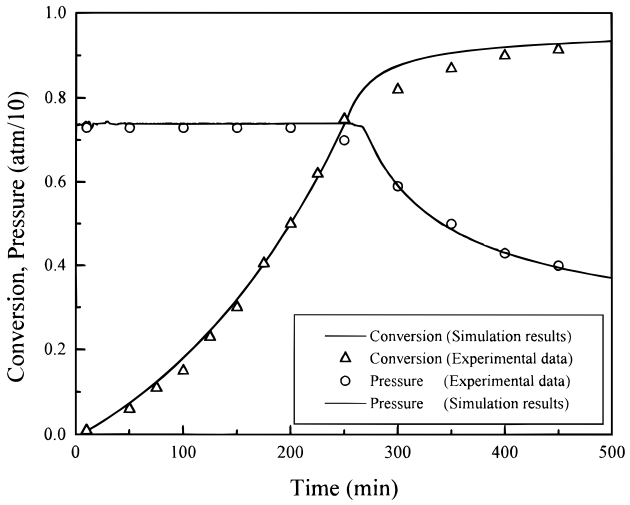

Figure 15. Comparison between theoretical model predictions and experimental results (Xie et al., 1991) on reactor pressure and monomer conversion. Experimental conditions: $T = 50$ °C, initiator Perkadox 16-W40, [I] = 0.175 wt %.

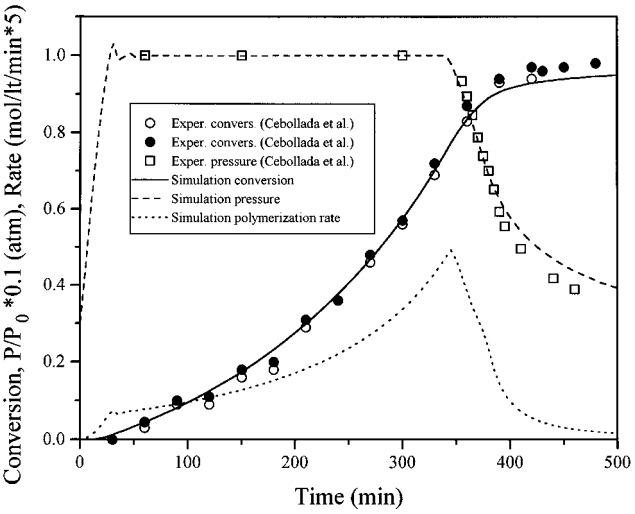

Figure 16. Comparison between theoretical model predictions and experimental results (Cebollada et al., 1989) on reactor pressure and monomer conversion. Experimental conditions: T = 60 °C; initiator, lauroyl peroxide (0.26 wt % based on monomer weight); initial mass of monomer, 10 kg; initial mass of water, 17 kg.

The predictive capabilities of the model presented in this paper were further tested by a direct comparison of model predictions with experimental data obtained from literature. Two different sources of experimental data were employed, namely, the one presented by Xie et al. (1991a−d) and the other by Cebollada et al. (1989). As can be seen, there is a good agreement between model predictions and experimental data on reactor pressure and monomer conversion (Figures 15 and 16). In Figure 17, model predictions on the variation of the average molecular weights with respect to monomer conversion are compared with the corresponding experimental data of Cebollada et al. (1989).

Based on the presented results, it can be claimed that a powerful dynamic model for the batch PVC suspension polymerization reactor has been developed. The next step is to use this model in order to optimize the PVC production. Some initial results concerning the optimization of industrial PVC reactors are presented next. From the results presented in Figure 5, it is obvious that, in a typical VCM suspension polymerization, a very sharp rate peak appears around the critical conversion, X_f. Industrial-scale reactors are designed with

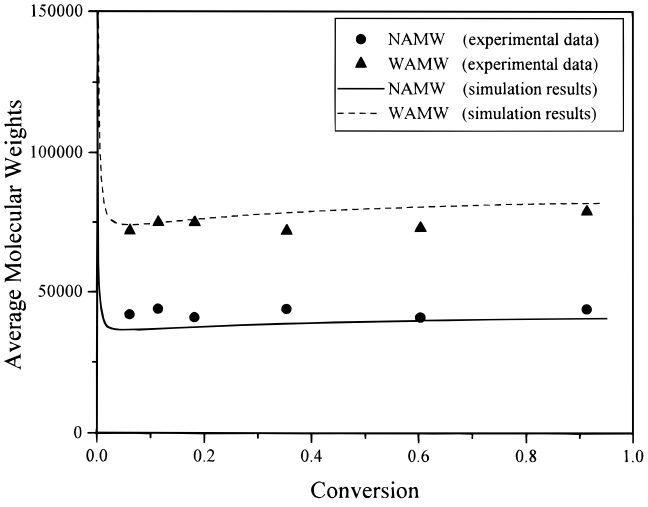

Figure 17. Comparison between theoretical model predictions and experimental results (Cebollada et al., 1989) on number- and weight-average molecular weight. Experimental conditions as in Figure 16.

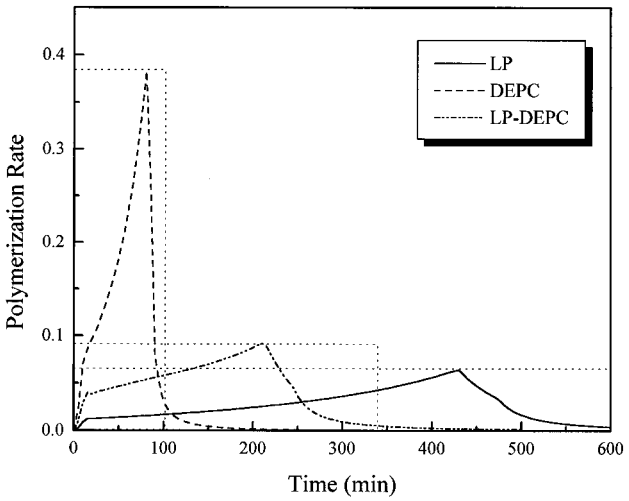

Figure 18. Polymerization rate versus time for a single initiator and a mixture of two initiators.

a maximum reactor cooling capacity corresponding to the maximum rate of heat release. In order to take full advantage of the reactor cooling capacity, the polymerization rate must be kept approximately constant at a level which yields a reaction heat rate equal to the maximum cooling capacity of the system. The common solution to this problem is to use a combination of rapid and slow initiators (Törnell, 1988). Other ways for the economization of the PVC production include the stagewise addition of the initiator, use of inhibitors (Grishin et al., 1992), optimal change of the reactor temperature during polymerization (nonisothermal conditions), etc. (Sidiropoulou and Kiparissides, 1996). To obtain a rectangular-like reaction rate profile, a mixture of a rapid and a slow initiator can be used. A comparison of the reaction rate profiles obtained by the two initiators used either alone or in combination is depicted in Figure 18. The total amount of initiator(s) in all experiments was kept constant, and all other experimental conditions were exactly the same. One way to quantify the flat reaction rate profile is to calculate the unused heat removal capacity (Cameron et al., 1981). The value of this quantity can be estimated by the difference between the maximum cooling capacity for which the reactor is designed (area of the dotted rectangular defined by the maximum reaction rate and the time at which a certain conversion occurs) and the heat actually removed (e.g., integral of the reaction rate versus time). From Figure 18 it can be seen that for the slow initiator a longer polymerization time and a smaller heat peak are observed, while the fast initiator shows an opposite behavior. On the other hand, from the point of improved heat removal and improved productivity, the combination of the two initiators is recommended.

Conclusions

In the present investigation a comprehensive mathematical framework is presented for modeling batch PVC suspension polymerization reactors. A detailed kinetic mechanism was considered and the general rate functions for the production of live and dead polymer chains were derived. Using the method of moments, several molecular and structural characteristics of the macromolecules (i.e., number- and weight-average molecular weight, number of SCB, LCB, and TDB) were calculated. Furthermore, detailed material balances were derived for the monomer distribution between the four phases (e.g., monomer-rich, polymer-rich, gaseous, and water) present in the reactor. Considering the reactor thermal requirements, energy balances were formulated for the reaction, jacket, and metal wall temperatures. Reactor pressure was calculated during the whole course of the reaction based on fundamental thermodynamic considerations. Expressions for diffusion-controlled termination and propagation rate constants were developed based on a fundamental model. The experimental part of this investigation included the operation of a lab-scale fully automated batch reactor. It was shown that experimental data on reactor temperature and pressure as well as on the jacket inlet and outlet temperature were in good agreement with the theoretical model predictions. Furthermore, the predictive capabilities of the present model were tested by comparison of the model predictions with experimental data reported by other laboratories. Finally, some results on the reactor economization were presented.

Nomenclature

A_{env} = reactor heat-transfer area to the environment, m^2
A_i = reactor inside heat-transfer area, m^2
A_o = reactor outside heat-transfer area, m^2
A_t = reactor top heat-transfer area, m^2
B_i = virial coefficient of a substance i
c_p = heat capacity, kJ/kg K
D = polydispersity index
D_{eq} = jacket equivalent diameter, m
DEPC = diethyl peroxydicarbonate
ΔH_r = specific reaction enthalpy, kJ/kmol
D_m = diffusion coefficient of the monomer, m^2/s
D_{imp} = impeller diameter, m
D_p = diffusion coefficient of the polymer, m^2/s
D_R = reactor inside diameter, m
E_{coh} = cohesive energy
$\hat{f}$ = fugacity, Pa
$f_{i,j}$ = efficiency of initiator i in the j phase
$F_{w,J}$ = water mass flow in jacket, kg/h
Gz = Graetz number
h_i = heat-transfer coefficient of the reaction mixture side, kJ/(m s K)
h_0 = heat-transfer coefficient from the reactor wall to jacket, kJ/(m s K)
$I_{i,j}$ = concentration of initiator i in the j phase, $kmol/m^3$
j_c = entanglement spacing
K = solubility constant for the VCM in the water phase
k = thermal conductivity, kW/K

k_{b_j} = intramolecular transfer rate constant in the j phase, 1/s
$k_{d_{i,j}}$ = decomposition rate constant of initiator i in the j phase, s^{-1}
k_{fm_j} = chain transfer to monomer rate constant in the j phase, m^3/(kmol s)
k_{fp_j} = chain transfer to polymer rate constant in the j phase, m^3/(kmol s)
$k_{I_{i,j}}$ = initiation rate constant of initiator i in the j phase, m^3/(kmol s)
k_{p_j} = propagation rate constant in the j phase, m^3/(kmol s)
k_{tc_j} = termination by combination rate constant in the j phase, m^3/(kmol s)
k_{td_j} = termination by disproportionation rate constant in the j phase, m^3/(kmol s)
$k_{t_j} = = k_{tc_j} + k_{td_j}$
k_{tD} = termination rate constant taking into account the effect of diffusion of polymer chains, m^3/(kmol s)
$k_{t,res}$ = residual termination rate constant in polymer phase, m^3/(kmol s)
k_{z_j} = inhibition rate constant in the j phase, m^3/(kmol s)
LCB = concentration of long-chain branches, kmol/m^3
L_d = number density of long-chain branches per 1000 monomer units
L_{eq} = jacket equivalent length, m
L_n = number of long-chain branches per polymer molecule
LP = lauroyl peroxide
M_0 = initial mass of VCM, kg
M_g = VCM mass in the gaseous phase
M_j = mass of VCM in the j phase, kg
M_{ji} = molecular weight of the jumping unit of monomer (i = m) or polymer (i = p)
M_n = number-average molecular weight, kg/kmol
M_w = weight-average molecular weight, kg/kmol
M_{wat} = VCM mass in the water phase
MWD = molecular weight distribution
MW_m = molecular weight of VCM, kg/kmol
MW_w = molecular weight of water, kg/kmol
N_A = Avogadro's number
N_d = number of initiators used
N_{imp} = agitator revolution number, rpm
P = total reactor pressure, Pa
P_m = VCM partial pressure, Pa
P_m^{sat} = VCM saturation pressure, Pa
Pr = Prandtl number
P_w = water partial pressure, Pa
P_x = concentration of dead polymer chains with x VCM units, kmol/m^3
R = ideal gas constant, J/mol/K
r_t, r_m = effective reaction radius for the termination and propagation, respectively
$R^\bullet_{n,j}$ = concentration of live polymer radicals with n VCM units in the j phase, kmol/m^3
Re = Reynolds number
SCB = concentration of short chain branches, kmol/m^3
S_d = number density of short-chain branches per 1000 monomer units
S_n = number of short-chain branches per polymer molecule
T = reactor mixture temperature, K
t = time, s
TDB = concentration of terminal double bonds, kmol/m^3
T_{env} = temperature of the environment surrounding the reactor, K
T_h = temperature equivalent of the thermocouple output, K
T_J = reactor's jacket temperature, K
T_{met} = temperature of the metal wall, K
T_n = number of terminal double bonds per polymer molecule
TNCLD = total number chain length distribution
U_{env} = heat-transfer coefficient to the reactor environment, kJ/(m s K)
U_t = heat-transfer coefficient from the reactor top, kJ/(m s K)
u_w = water velocity in the jacket, m/s
VCM = vinyl chloride monomer
V_f = free volume of the mixture
V_g = volume of the gaseous phase, m^3
$\hat{V}_i^*$ = specific critical volume of substance i, m^3/g
V_J = jacket volume, m^3
V_{met} = metal wall volume, m^3
V_{mix} = reaction mixture volume, m^3
V_R = reactor volume, m^3
W_w = total mass of water introduced in the reactor, kg
W_{wl} = water mass in the liquid phase, kg
X = monomer conversion
X_{c0} = critical degree of polymerization for entanglements of the pure polymer
X_f = critical conversion at which the monomer phase disappears
X_n = number-average chain length
Z_j = inhibitor concentration in the j phase, kmol/m^3

Greek Symbols

α_i = activity of a substance i
γ = overlap factor
δ = average root-mean-square end-to-end distance per square root of the number of monomer units in a chain
δ_i = solubility parameter of the i component
$\lambda_{i,j}$ = ith moment of molecular weight distribution of live polymer radicals in the j phase
μ_κ = kth moment of dead polymer chains
ξ = ratio of the critical molar volume of the jumping unit to the critical molar volume of the polymer
ρ_g = density of the gaseous phase, kg/m^3
ρ_m = monomer density, kg/m^3
ρ_{met} = metal wall density, kg/m^3
ρ_p = polymer density, kg/m^3
ρ_w = water density, kg/m^3
φ_i = volume fraction of species i
$\hat{\varphi}$ = fugacity coefficient
χ = Flory−Huggins interaction parameter
ω = weight fraction

Subscripts

c = critical
g = gaseous phase
m = monomer phase
p = polymer phase
w = water phase

Superscripts

m = monomer phase
p = polymer phase
g = gaseous phase
w = water phase

Appendix. Thermodynamic Calculations and Physical Properties

In this appendix the calculations of the thermodynamic and physical properties, required for the simulation of a batch VCM suspension polymerization reactor, are detailed. The estimation of monomer distribution between different phases and the calculation of the Flory−Huggins interaction parameter are of significant importance in the VCM suspension polymerization. Furthermore, the dependence of thermodynamic and physical properties (i.e., density, viscosity, specific heat, and thermal conductivity) on temperature and composition must be known in any comprehensive modeling study.

The virial coefficients of a pure substanc, B_i, and of a binary mixture, B_{ij}, are related to the accentric factors

ω_i and ω_{ij}, respectively:

$$B_i = \frac{RT_{c,i}}{P_{c,i}}(B_i^0 + \omega_i B_i^1); \qquad B_{ij} = \frac{RT_{c,ij}}{P_{c,ij}}(B_{ij}^0 + \omega_{ij} B_{ij}^1) \tag{A.1}$$

The values of B^0 and B^1 can be expressed in terms of the reduced temperature, T_r ($T_r = T/T_c$):

$$B_i^0 = 0.083 - \frac{0.422}{T_{r,i}^{1.6}}; \qquad B_i^1 = 0.139 - \frac{0.172}{T_{r,i}^{4.2}} \tag{A.2}$$

The pseudocritical properties of a pair ($i-j$) of components are given by the following equations:

$$\omega_{ij} = \frac{\omega_i + \omega_j}{2}; \qquad T_{c,ij} = (T_{c,i}T_{c,j})^{1/2};$$

$$P_{c,ij} = \frac{Z_{c,ij}RT_{c,ij}}{V_{c,ij}} \tag{A.3}$$

where

$$Z_{c,ij} = \frac{Z_{c,i} + Z_{c,j}}{2}; \qquad V_{c,ij} = \left(\frac{V_{c,i}^{1/3} + V_{c,j}^{1/3}}{2}\right)^3 \tag{A.4}$$

Calculation of the Flory−Huggins Interaction Parameter, χ. The Flory−Huggins interaction parameter, χ, can be expressed as the sum of an enthalpic, entropic, and interfacial contribution (Nilsson et al., 1978):

$$\chi = \chi_H + \chi_S + \chi_I \tag{A.5}$$

The enthalpic contribution to the interaction parameter can be calculated in terms of the solubility parameters, δ_1 and δ_2, from the following expression:

$$\chi_H = \frac{V_1((\delta_1 - \delta_2)^2 + 2\delta_1\delta_2 l_{12})}{RT} \tag{A.6}$$

In the above expression V_1 stands for the molar volume of the solvent (i.e., VCM) in the polymer solvent mixture. According to the experimental results of Nilsson et al. (1978), the interaction parameter, χ, depends on the polymer volume fraction, φ_2, and the polymerization temperature. As a result, these two factors should be included in the calculation of the interaction parameter, χ, through the introduction of an appropriate expression for the calculation of l_{12}. Such an expression can have the following form:

$$l_{12} = a + b\varphi_2^2 + c\varphi_2 + d/T \tag{A.7}$$

where T is the reaction temperature and a, b, c, and d are adjustable parameters which were calculated by fitting experimental data on the swelling of PVC with VCM (Nilsson et al., 1978). The suggested values are $a = 0.155\,24$, $b = 0.353\,11$, $c = -0.505\,27$, and $d = 11.3605$.

The entropic contribution χ_S, has been found to have a value between 0.2 and 0.3 for many polymer−solvent systems. A value of 0.26 is used in this investigation. For the suspension polymerization, since the radius of the particles is large enough, the interfacial contribution, χ_I, to the interaction parameter can be neglected.

Calculation of the Solubility Parameters. The solubility parameters of the polymer and solvent, δ_2 and δ_1, respectively, as well as the VCM molar volume, V_1, can be calculated from the group contribution theory. The solubility parameter, δ, is equal to the square root of the ratio of the cohesive energy, E_{coh}, over the solvent molar volume, V_1:

$$\delta_1 = \sqrt{\frac{E_{coh_1}}{V_1}} \tag{A.8}$$

Based on the group contribution theory, the cohesive energy and the molar volume for VCM were calculated: $E_{coh_1} = 20\,170$ J/mol and $V_1 = 66$ cm^3/mol. As a result, the solubility parameter was computed: $\delta_1 = 17.481$ J$^{1/2}$/cm$^{3/2}$.

For calculation of the polymer solubility parameter, δ_2, indirect methods were employed. The contributions of dispersive forces, δ_D, hydrogen bonding, δ_H, and polar forces, δ_P, were introduced in order to estimate the cohesive energy and δ_2:

$$E_{coh_2} = E_D + E_H + E_P \Rightarrow \delta_2^2 = \delta_D^2 + \delta_H^2 + \delta_P^2 \tag{A.9}$$

For the PVC/VCM system, the calculated value of δ_2 was $\delta_2 = 22.5$ J$^{1/2}$/cm$^{3/2}$.

Physical Properties of the Polymerizing Mixture.

Density of the droplet:

$$\rho_d = \left(\frac{1 - x}{\rho_m} + \frac{x}{\rho_p}\right)^{-1} \tag{A.10}$$

Density of the suspension mixture:

$$\rho_{mix} = \rho_w\varphi_w + \rho_d(1 - \varphi_w) \tag{A.11}$$

Viscosity of suspension:

$$\mu_{mix} = \mu_w[1 + 2.5\varphi_p + 7.54\varphi_p^2] \tag{A.12}$$

Heat capacity of suspension:

$$c_{p_{mix}} = \sum \xi_i c_{p_i} = \xi_w c_{p_w} + \xi_{VCM} c_{p_{VCM}} + \xi_{PVC} c_{p_{PVC}} \tag{A.13}$$

Thermal conductivity of suspension:

$$k_{mix} = \frac{k_w[2k_w + k_{PVC} - 2\varphi_p(k_w - k_{PVC})]}{2k_w + k_{PVC} + \varphi_p(k_w - k_{PVC})} \tag{A.14}$$

Literature Cited

Abdel-Alim, A. H.; Hamielec, A. E. Bulk Polymerization of Vinyl Chloride. *J. Appl. Polym. Sci.* **1972**, *16*, 783.

Achilias, D. S.; Kiparissides, C. Development of a General Mathematical Framework for Modelling Diffusion-Controlled Free-Radical Polymerization Reactions. *Macromolecules* **1992**, *25*, 3739.

Achilias, D. S.; Kiparissides, C. On the Validity of the Steady-State Approximations in High-Conversion Diffusion-Controlled Free-Radical Copolymerization Reactions. *Polymer* **1994**, *35* (8), 1714.

Arriola, D. J. Mathematical Modelling of Addition Polymerization Reactions. Ph.D. Dissertation, University of Wisconsin, Madison, WI, 1989.

Baltsas, A.; Achilias, D. S.; Kiparissides, C. A Theoretical Investigation of the Production of Branched Copolymers in Continuous Stirred Tank Reactors. *Macromol. Theory Simul.* **1996**, *5*, 477.

Bevis, M. J. Looking to the Future. *World Plast. Rubber Technol.* **1996**, *8*, 77.

Bretelle, D.; Machietto, S. Dynamic Simulation of a PVC Batch Reactor. *ESCAPE-2* **1994**, S317−S322.

Buback, M.; Huckenstein, B.; Russell, G. T. Modelling of Termination in Intermediate and High Conversion Free Radical Polymerizations. *Macromol. Chem. Phys.* **1994**, *195*, 539.

Burgess, R. H. *Manufacturing and Processing of PVC*; Applied Science Publishers: London, 1982.

Cameron, J. B.; Lundeen, A. J.; McCulley, J. M.; Schwab, P. A. Trends in Suspension PVC Manufacture. *J. Appl. Polym. Sci., Appl. Polym. Symp.* **1981**, *36*, 133.

Cebollada, A. F.; Schmidt, M. J.; Farber, J. N.; Capiati, N. J.; Valles, E. M. Suspension Polymerization of Vinyl Chloride. *J. Appl. Polym. Sci.* **1989**, *37*, 145.

Chan, R. K. S.; Langsam, M.; Hamielec, A. E. Calculation and Applications of VCM Distribution in Vapor/Water/Solid Phases during VCM Polymerization. *J. Macromol. Sci., Chem.* **1982**, *A17* (6), 969.

Daupert, T. E.; Danner, R. P. Data Compilation Tables of Properties of Pure Compounds. *Design Insitute for Physical Properties Data*; AIChE: New York, 1985.

Dimian, A.; van Diepen, D.; van der Wal, G. A. Dynamic Simulation of a PVC Suspension Reactor. *Comput. Chem. Eng.* **1995**, *19S*, S427.

Ferry, J. D. *Viscoelastic Properties of Polymers*, 3rd ed.; Wiley-Interscience: New York, 1980.

Grishin, A. N.; Zegelman, V. I.; Fomin, V. A.; Etlis, I. V.; Popov, V. A.; Khavritsyn, V. In *4th International Workshop on Polymer Reaction Engineering;* Reichert, K. H., Moritz, H. U., Eds.; VCH: Weinheim, Germany, 1992; Vol. 127, p 449.

Hamielec, A. E.; Gomez-Vaillard, R.; Marten, F. L. Diffusion-Controlled Free Radical Polymerization. Effect on Polymerization Rate and Molecular Properties of PVC. *J. Macromol. Sci., Chem.* **1982**, *A17* (6), 1005.

Kelsall, D. C.; Maitland, G. C. The Interaction of Process Conditions and Product Properties for PVC. In *Polymer Reaction Engineering;* Reichert, K. H., Geiseler, W., Eds.; VCH Publishers: Berlin, 1983; p 133.

Kiparissides, C.; Shah, S. L. Self-tuning and Stable Adaptive Control of a Batch Polymerization Reactor. *Automatica* **1983**, *19* (3), 225.

Kuchanov, S. I.; Bort, G. C. Kinetics and Mechanism of Bulk Polymerization of Vinyl Chloride. *Polym. Sci. USSR* **1973**, *A15*, 2712.

Langsam, M. In *Encyclopedia of PVC*, 2nd ed.; Nass, L. I., Heiberger, C. A., Eds.; Marcel Dekker Inc.: New York and Basel, 1986; Vol. 1, p 48.

Lewin, D. R. Modelling and Control of an Industrial PVC Suspension Polymerization Reactor. *Comput. Chem. Eng.* **1996**, *20*, S865.

Litvinenko, G. I.; Kaminsky, V. A. Role of Diffusion-Controlled Reactions in Free-Radical Polymerization. *Prog. React. Kinet.* **1994**, *19*, 139.

Nilsson, H.; Silvegren, C.; Törnell, B. Swelling of PVC Latex Particles by VCM. *Eur. Polym. J.* **1978**, *14*, 737.

Panke, D. Modelling the Free-Radical Polymerization of MMA over the Complete Range of Conversion. *Macromol. Theory Simul.* **1995**, *4*, 759.

Pertsinidis, A.; Papadopoulos, E.; Kiparissides, C. Computer Aided Design of Polymer Reactors. *ESCAPE-96*, Rhodes, Greece, May 1996.

Ray, W. H.; Jain, S. K.; Salovey, R. On the Modelling of Bulk PVC Reactors. *J. Appl. Polym. Sci.* **1975**, *19*, 1297.

Scherrenberg, R. L.; Reynaers, H.; Gondard, C.; Booij, M. Structural Aspects of Suspension PVC. *J. Polym. Sci., Polym. Phys.* **1994**, *32*, 99.

Sidiropoulou, E.; Kiparissides, C. Mathematical Modelling of PVC Suspension Polymerization. *J. Macromol. Sci., Chem.* **1990**, *A27* (3), 257.

Sidiropoulou, E.; Kiparissides, C. Temperature and Initiator Policies for Constant Rate Suspension Polymerization of Vinyl Chloride. **1997**, in preparation.

Smallwood, P. V. Vinyl Chloride Polymers, Polymerization. In *Encyclopedia of Polymer Science and Technology;* Mark, H., Ed.; Wiley: New York, 1990; Vol. 17, p 295.

Tefera, N.; Weickert, G.; Bloodworth, R.; Schweer, J. Free Radical Suspension Polymerization Kinetics of Styrene up to High Conversion. *Macromol. Chem. Phys.* **1994**, *195*, 3067.

Törnell, B. E. Recent Developments in PVC Polymerization. *Polym. Plast. Technol. Eng.* **1988**, *27*, 1.

Ugelstad, J.; Moerk, P. C.; Hansen, F. K.; Kaggerund, K. H.; Ellingsen, T. Kinetics and Mechanism of Vinyl Chloride Polymerization. *Pure Appl. Chem.* **1981**, *53*, 323.

Voutetakis, P. Design and Control of a Batch Polymerization Reactor. Ph.D. Dissertation, Aristotle University of Thessaloniki, Thessaloniki, Greece, 1992.

Weickert, G.; Henschel, G.; Weissenborn, K.-D. Kinetik der VC Polymerisation. Ein Modellvergleich I. *Angew. Makromol. Chem.* **1987a**, *147*, 1.

Weickert, G.; Henschel, G.; Weissenborn, K.-D. Kinetik der VC Polymerisation. Ein Modellvergleich II. *Angew. Makromol. Chem.* **1987b**, *147*, 19.

Weickert, G.; Klodt, R.-D.; Platzer, B.; Weissenborn, K.-D.; Henschel, I. Ein Modell zur quantitativen Beschreibung der Morphogenesis von PVC-S, I. *Angew. Makromol. Chem.* **1988a**, *164*, 59.

Weickert, G.; Platzer, B.; Weissenborn, K.-D.; Klodt, R.-D.; Henschel, I. Ein Modell zur quantitativen Beschreibung der Morphogenesis von PVC-S, II. *Angew. Makromol. Chem.* **1988b**, *164*, 79.

Xie, T. Y.; Hamielec, A. E.; Wood, P. E.; Woods, D. R. *J. Appl. Polym. Sci.* **1987**, *34*, 1749.

Xie, T. Y.; Hamielec, A. E.; Wood, P. E.; Woods, D. R. Suspension, Bulk and Emulsion Polymerization of Vinyl Chloride—Mechanism, Kinetics and Reactor Modelling. *J. Vinyl Technol.* **1991a**, *13* (1), 2.

Xie, T. Y.; Hamielec, A. E.; Wood, P. E.; Woods, D. R. Experimental Investigation of Vinyl Chloride Polymerization at High Conversion: Mechanism, Kinetics and Modelling. *Polymer* **1991b**, *32* (3), 537.

Xie, T. Y.; Hamielec, A. E.; Wood, P. E.; Woods, D. R. Experimental Investigation of Vinyl Chloride Polymerization at High Conversion: Molecular Weight Development. *Polymer* **1991c**, *32* (6), 1098.

Xie, T. Y.; Hamielec, A. E.; Wood, P. E.; Woods, D. R. Experimental Investigation of Vinyl Chloride Polymerization at High Conversion: Reactor Dynamics *J. Appl. Polym. Sci.* **1991d**, *43*, 1259.

Yuan, H. G.; Kalfas, G.; Ray, W. H. Suspension Polymerization. *J. Macrom. Sci., Rev. Macromol. Chem. Phys.* **1991**, *C31* (2 & 3), 215.

Received for review August 6, 1996
Revised manuscript received November 8, 1996
Accepted November 13, 1996[⊗]

IE9604839

[⊗] Abstract published in *Advance ACS Abstracts,* February 15, 1997.